



Integrated proteomic, phosphoproteomic, and N-glycoproteomic analyses of the *longissimus thoracis* of yaks

Xinping Chang^a, Jiamin Zhang^a, Zhendong Liu^{b,c}, Zhang Luo^{b,c,**}, Lin Chen^a, Jinqiu Wang^a, Fang Geng^{a,*}

^a Meat Processing Key Laboratory of Sichuan Province, School of Food and Biological Engineering, Chengdu University, Chengdu, 610106, China

^b Provincial and Ministerial Co-Founded Collaborative Innovation Center for R & D in Tibet Characteristic Agricultural and Animal Husbandry Resources, Tibet Agricultural and Animal Husbandry University, Linzhi, 860000, China

^c College of Food Science, Tibet Agricultural and Animal Husbandry University, Linzhi, 860000, China

ARTICLE INFO

Handling Editor: Dr. Yeonhwa Park

Keywords:

Yak
Meat
LC-MS/MS
Proteome
N-glycoproteome

ABSTRACT

Yaks (*Bos mutus*) live in the Qinghai–Tibet plateau. The quality of yak meat is unique due to its genetic and physiological characteristics. Identification of the proteome of yak muscle could help to reveal its meat-quality properties. The common proteome, phosphoproteome, and N-glycoproteome of yak *longissimus thoracis* (YLT) were analyzed by liquid chromatography-tandem mass spectrometry-based shotgun analysis. A total of 1812 common proteins, 1303 phosphoproteins (3918 phosphorylation sites), and 204 N-glycoproteins (285 N-glycosylation sites) were identified in YLT. The common proteins in YLT were involved mainly in myofibril structure and energy metabolism; phosphoproteins were associated primarily with myofibril organization, regulation of energy metabolism, and signaling; N-glycoproteins were engaged mainly in extracellular-matrix organization, cellular immunity, and organismal homeostasis. We reported, for the first time, the “panorama” of the YLT proteome, specifically the N-glycoproteome of YLT. Our results provide essential information for understanding *post mortem* physiology (rigor mortis and aging) and the quality of yak meat.

1. Introduction

The yak (*Bos mutus*) has adaptability to high altitudes. The muscles of yaks differ markedly in structure and physiology from those of plain cattle so that they can adapt to low-oxygen environments (Gu et al., 2021; Wang et al., 2011). These physiological differences result in significant differences in post-slaughter physiological processes in yak meat (Wang et al., 2014; Xin et al., 2019). The differences in the fiber structure and physiology of muscle give yak meat unique processing properties and edible qualities (Wang et al., 2022; Yang et al., 2021; Zuo et al., 2016). Protein is crucial to shaping the structure and dominates the physiology of muscle. Therefore, the type of muscle protein in yaks is fundamental for understanding the mechanism of *post mortem*

physiology and the processing properties of yak meat.

Proteomic analysis enables high-throughput identification and analyses of proteins in biological samples (Cao et al., 2022). It has become a powerful tool for elucidating the underlying molecular mechanisms of meat quality (Antonelo et al., 2022; Kemp and Parr, 2012; López-Pedrouso et al., 2021). For example, isobaric tags for relative and absolute quantification (iTRAQ) proteomic analysis has shown 20 proteins to be more abundant and 30 to be less abundant in the *longissimus thoracis* of yaks than in the *longissimus thoracis* of cattle (Wen et al., 2019). This differential abundance of proteins is associated with molecular functions such as binding, catalytic activity, and structural activity. Such information provides important clues to further elucidate the mechanism of high-altitude adaptation in yaks at the muscle-cell

Abbreviations: YLT, yak *longissimus thoracis*; iTRAQ, isobaric tags for relative and absolute quantification; LC-MS/MS, liquid chromatography-tandem mass spectrometry; RPLC, reverse-phase liquid chromatography; UPLC, ultra-high-pressure liquid chromatography; IMAC, immobilized metal affinity chromatography; HILIC, hydrophilic interaction liquid chromatography; GO, Gene Ontology; KEGG, Kyoto Encyclopedia of Genes and Genomes; KOG, Eukaryotic Orthologous Groups; MF, molecular function; BP, biological processes; CC, cellular components; ECM, extracellular matrix.

* Corresponding author.

** Corresponding author. Provincial and Ministerial Co-Founded Collaborative Innovation Center for R & D in Tibet Characteristic Agricultural and Animal Husbandry Resources, Tibet Agricultural and Animal Husbandry University, Linzhi, 860000, China.

E-mail addresses: luozhang1759@xza.edu.cn (Z. Luo), gengfang@cdu.edu.cn (F. Geng).

<https://doi.org/10.1016/j.crf.2022.09.012>

Received 28 May 2022; Received in revised form 27 August 2022; Accepted 12 September 2022

Available online 13 September 2022

2665-9271/© 2022 The Authors. Published by Elsevier B.V. This is an open access article under the CC BY-NC-ND license (<http://creativecommons.org/licenses/by-nc-nd/4.0/>).

level. In the previous study, quantitative proteomic analysis of tenderloins between Tibetan pigs and Yorkshire pigs showed that 171 proteins were different in terms of abundance (Gu et al., 2019). These differentially abundant proteins were involved mainly in energy production, glutathione metabolism, muscle contraction, immunity and defense, and closely related to the edible quality of pork.

The physiological functions and physicochemical properties of proteins are closely related to their post-translational modification. Thus, besides the type and abundance of proteins, the modifications of proteins have been the focus of attention in recent years, especially the phosphorylation of proteins associated with meat consumption. Zhang's team (Chen et al., 2019a; Chen et al., 2018; Li et al., 2017) reported the phosphoproteomic analysis of lambs, and found that phosphoproteins play an important role in the meat quality formation of lamb during the post-mortem process. In addition to phosphorylation, glycosylation is involved in biological processes that affect the structure and physiological function of proteins. O-glycoproteome is difficult to analyze in high-throughput analysis due to its complexity, so only the N-glycoproteome has been studied extensively. (Cao et al. 2017) employed quantitative N-glycoproteomics analysis to identify 110 and 91 N-glycosites from human colostrum and mature milk, respectively. They found that N-glycoproteins with different levels of N-glycosylation were associated with processes within the immune system. Similarly, differential abundance of N-glycosylated proteins was found to be involved in the immune system when comparing the glycoproteomes between human milk and bovine milk (Cao et al., 2019). Compared with milk, the 13 N-glycoproteins (containing 13 N-glycosides) in yogurt were significantly changed after the fermentation (Xiao et al., 2022). Previously, 26 N-glycoproteins (71 glycosylation sites) were identified in egg white and 86 N-glycoproteins (217 glycosylation sites) in egg yolk, and further elucidated the importance of glycosylation modifications on the structural function, bioactivity and allergenicity of egg proteins (Geng et al., 2017, 2018). Furthermore, Liu and colleagues found that spray-drying changed the functional properties of egg white to some extent during different heat treatments (Liu et al., 2021).

Although the proteome and phosphoproteome of yak meat have been reported, the N-glycoproteome has not been identified or analyzed, and complete knowledge of the proteomes in yak meat is lacking. Therefore, in the present study, the proteome, phosphoproteome, and N-glycoproteome of yak *longissimus thoracis* (YLT) were analyzed by “shotgun analyses”. To improve the throughput of liquid chromatography-tandem mass spectrometry (LC-MS/MS) identification, the YLT peptides obtained by trypsin digestion were first fractionated by high-pH reverse-phase liquid chromatography (RPLC), which increased the number of identified proteins. Bioinformatics analysis was done based on the identified YLT proteins to elucidate the potential roles of phosphoproteins and N-glycoproteins in the *post mortem* rigor mortis and aging of YLT.

2. Materials and methods

2.1. Sample collection

Six yaks (18–24 months) were selected from pastures in Bayi District (Linzhi City, Tibet Autonomous Region). After 12 h of fasting, they were electrocuted and killed at a local slaughterhouse. After slaughter (20–30 min after electrical stimulation), muscle samples from the anterior middle section of YLT were collected and divided into samples of weight ~15 g. Then, the samples were frozen immediately in liquid nitrogen and stored at -80°C until analyses.

2.2. Extraction and digestion of proteins

For the extraction and digestion of proteins, two replicates for each YLT sample were used to ensure the reproducibility of protein analyses. The workflow for proteomics, phosphoproteomics, and N-

glycoproteomics analysis comprised five main steps (Graphical Abstract): extraction and digestion of YLT protein; offline high-pH RPLC fractionation; enrichment of phosphopeptides and glycopeptides; LC-MS/MS identification; bioinformatics analysis.

YLT proteins were extracted and digested with reference to a method described previously (Liu et al., 2021; Xiao et al., 2022). First, YLT (10 g) was ground into a powder in liquid nitrogen and mixed with 40 mL of lysis buffer (urea (8 mol/L), 1% protease inhibitor mixture, and dithiothreitol (10 mmol/L)) in a tube. Then, three ultrasonic extractions (150 W, 30-s each) were carried out on ice using a high-intensity ultrasound processor (JY92-II; Ningbo Scientz Biotechnology, Ningbo, China). After centrifugation ($12000\times g$ for 10 min at 4°C), the supernatant was collected and transferred to a clean tube. The protein concentration was determined using a Bicinchoninic Acid Protein Assay Kit (P0010; Biyu Biotechnology Institute, Shanghai, China).

The samples of extracted total protein were reduced sequentially with dithiothreitol (5 mmol/L) at 56°C for 30 min, and then alkylated with iodoacetamide (11 mmol/L) for 15 min in the dark at room temperature. Then, triethylamine borane (100 mmol/L) was added to dilute the sample so that the urea concentration was <2 mol/L. YLT samples were digested at a mass ratio of trypsin: protein of 1:50 in the first digestion (overnight) and at 1:100 in the second digestion (4 h).

2.3. Offline high-pH RPLC fractionation

The samples of mixed peptides (2 replicates \times 6 YLT) were separated by a modified offline high-pH RPLC fractionation protocol with a BetaSil™ C18 column (5 μm , 10×250 mm) equipped on an Acquity ultra-high-pressure liquid chromatography (UPLC) system (Waters, Milford, MA, USA) (Wang et al., 2019; Yang et al., 2012). Briefly, the peptide was first separated in a gradient of 8%–32% acetonitrile (pH 9.0) for 60 min and combined randomly into 14 fractions (for common proteome analysis), six fractions (for phosphoproteome analysis), or four fractions (for N-glycoproteome analysis). The acquired fractions were concentrated by vacuum centrifugation (RVC 2–25; Christ, Osterode am Harz, Germany) for further analyses.

2.4. Enrichment of phosphopeptides and N-glycopeptides

Immobilized metal affinity chromatography (IMAC) was used to enrich the phosphopeptides from the six fractions of YLT. Briefly, the peptide samples were dissolved using an enrichment buffer (50% acetonitrile and 6% trifluoroacetate) and the resulting samples were incubated with a pre-washed TiO_2 filler on a shaker (GL Sciences, Torrance, CA, USA). Then, three washes were undertaken using enrichment buffer and wash buffer (30% acetonitrile and 0.1% trifluoroacetate) to remove the unbound peptides, respectively. Next, the phosphopeptides were eluted using elution buffer (10% NH_3), vacuum freeze-dried, and desalted with C18 ZipTips (Millipore, Billerica, MA, USA), vacuum freeze-dried, and analyzed by LC-MS/MS.

Glycopeptides were enriched from the four fractions of YLT by hydrophilic interaction liquid chromatography (HILIC). The dried peptide fractions were reconstituted in 40 μL of enrichment buffer (80% acetonitrile and 1% trifluoroacetic acid) and then transferred to a HILIC microcolumn (Dalian Institute of Chemical Physics, Dalian, China). The HILIC microcolumn was centrifuged at $4000\times g$ for 15 min at 4°C . The glycopeptides were combined with HILIC filler and retained. Unbound peptides were washed thrice using an enrichment buffer. Then, the glycopeptides were eluted with 10% acetonitrile and lyophilized. Subsequently, the glycopeptides were resolved in 50 μL of H_2^{18}O , and deglycosylation was undertaken by addition of 2 μL of PNGase F (200 units; Roche, Basel, Switzerland) and incubated overnight at 37°C . Finally, the deglycosylated N-glycopeptides were desalted by C18 ZipTips, vacuum freeze-dried, and analyzed by LC-MS/MS.

2.5. LC-MS/MS

LC-MS/MS was undertaken using a Q Exactive™ plus mass spectrometer with an EASY-nLC 1000 UPLC system (Thermo Fisher Scientific, Waltham, MA, USA). Peptide samples were dissolved in solvent A (0.1% formic acid and 2% acetonitrile in water) and loaded onto a Resproil-Pur C18 reversed-phase analytical column (particle size = 1.9 μm, inner diameter = 75 μm, length = 15 cm). Solvent B was increased from 4% to 22% (0.1% formic acid, 98% acetonitrile) in 38 min, 22%–32% in 14 min, 80% in 4 min, and then kept at 80% for the final 4 min. The constant flow rate for the separation was 700 nL/min. After

separation, the sample was ionized by a nanoelectrospray ionization source (2000 V), then full-scan MS was carried out in a mass range of m/z 350 ± 1800 with a resolution of 70000. Mass spectra were acquired and the 20 most abundant peptides in the mass spectral data were analyzed by high-energy collisional decomposition (Geng et al., 2019a; Geng et al., 2019b; Liu et al., 2020a).

The obtained MS/MS data were processed by MaxQuant (www.maxquant.org/) and we searched for matches for *Bos mutus* with UniProt (www.uniprot.org/). We set 20 ppm as the value for the mass tolerance of the precursor ion in the first search, 5 ppm was set for the main search, and the set value for the mass tolerance of the fragment ion was 0.02 Da.

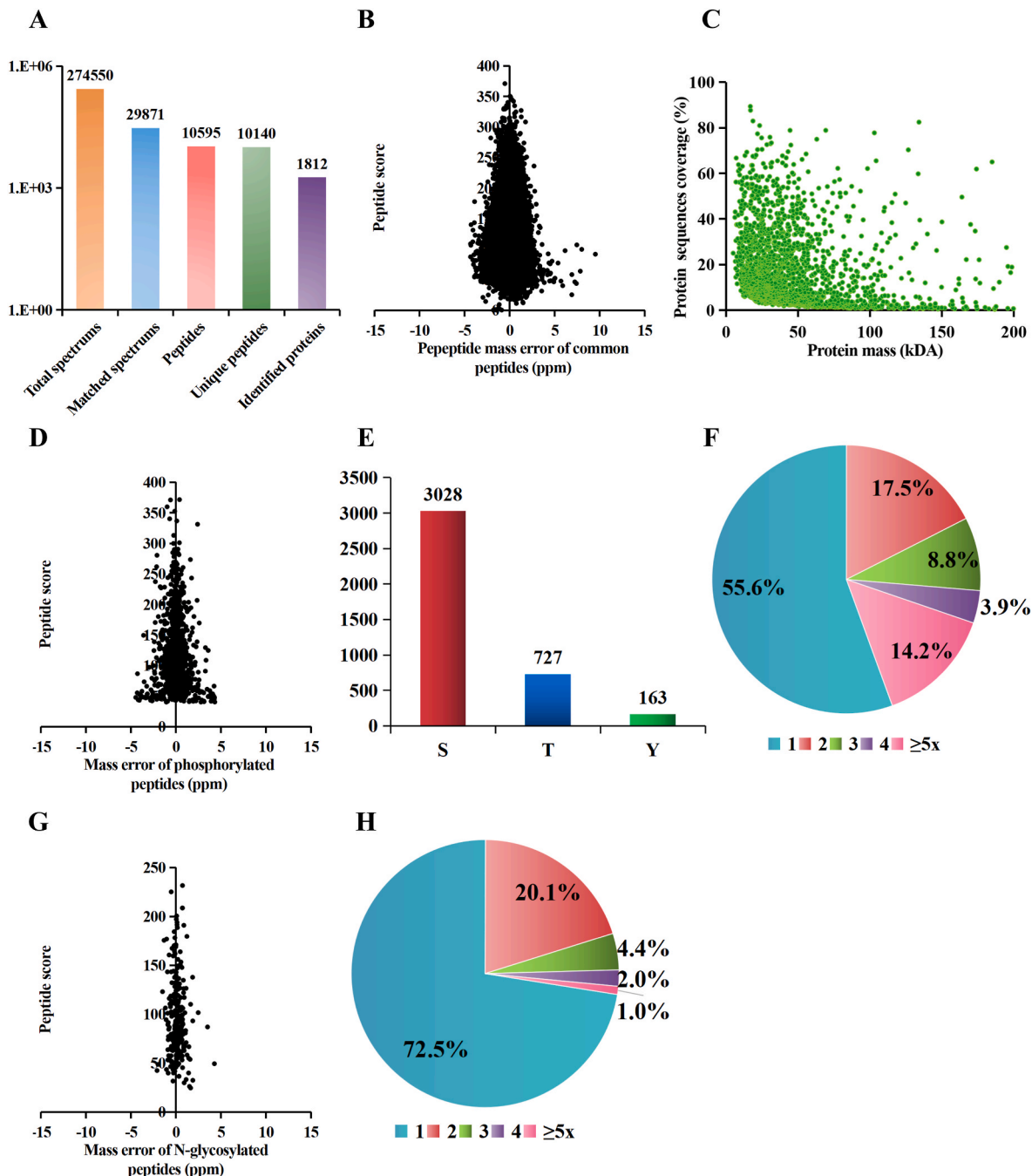


Fig. 1. Characterization of identified proteins, phosphorylation/N-glycosylation sites, peptides, and proteins in yak *longissimus thoracis*. (A) Statistical information of tandem mass spectra and protein identification; (B) mass error of identified common peptides; (C) length distribution of identified common peptides; (D) mass error of identified phosphorylated peptides; (E) number of phosphorylation sites in serine [S], threonine [T], and tyrosine [Y]; (F) number of phosphorylation sites of identified phosphorylated proteins; (G) number of identified N-glycosylated peptides with mass error; (H) number of N-glycosylation sites of identified N-glycoproteins.

The carbamidomethyl group of Cys was designated as a fixed modification, and acetylation on the N-terminal of the protein and oxidation of Met were designated as variable modifications. In addition, $^{18}\text{O}(\text{N})$ on asparagine was set as a variable modification for searching N-glycopeptides. Phosphorylation of serine, threonine, and tyrosine was set as a variable modification for searching phosphopeptides. The threshold for the false discovery rate for peptides, proteins, and modification sites was set at 1%.

2.6. Bioinformatics analysis

Motif-x (<http://meme-suite.org/tools/motif-x>) was used to seek modification motifs and all identified protein sequences were used as background; the incidence was set to 20 and other parameters were set to default values. Subcellular localization of the identified proteins was identified using Wolf PSORT at default settings (www.genscript.com/psort/wolf_psort.html).

Gene Ontology (GO) annotations of the identified proteins were obtained from the UniProt-Gene Ontology annotation database (www.ebi.ac.uk/GOA/). The identified protein IDs were first converted to UniProt IDs and then mapped to GO IDs. For proteins identified in the UniProt-GOA database that did not match the annotated proteins, InterPro (www.ebi.ac.uk/interpro/) was used to carry out GO annotation based on the method of protein-sequence matching. Upon GO analysis, a two-tailed Fisher's exact test was used to detect the degree of enrichment of the identified modified proteins for all proteins in the species database, and the corrected GO terms were considered significant at $P < 0.05$. The Kyoto Encyclopedia of Genes and Genomes (KEGG) database was used to annotate the pathways in which the identified proteins were involved. KEGG database-related descriptions of proteins were annotated using the KAAS service tool. Enriched KEGG pathways were mapped based on annotation information from the KEGG mapper tool.

3. Results and discussion

3.1. Common proteome of YLT

A total of 10595 peptides were identified from the common proteomic analysis of YLT (Fig. 1A). All peptides were identified with high precision and mass tolerance < 5 ppm for peptide ions (Fig. 1B). The identified peptides were of quality-controlled length, and distributed between 7 amino acids and 19 amino acids. Most of the identified proteins in YLT had a molecular-weight distribution between 20 kDa and 80 kDa, with $\sim 60\%$ of the coverage reaching $> 10\%$ (Fig. 1C), which indicated a high quality of protein identification. After removing repetitive sequences, 1812 common proteins were identified in YLT (Table S1). According to the protein abundance metric (PSM: protein matching spectral number), 18 of all identified YLT common proteins had PSM higher than 1%, mainly including proteins associated with muscle structure (myosin, actin, α -actinin, etc.) and some enzymes involved in energy metabolism (fructose-bisphosphate aldolase, creatine kinase and α -1,4 glucan phosphorylase, etc.), while these high abundance proteins were similar to those previously reported in yak proteomics (Wen et al., 2019; Zuo et al., 2016).

3.2. Phosphoproteome of YLT

IMAC-enriched YLT phosphopeptides were identified by LC-MS/MS. A total of 4306 peptides were identified, of which 3575 were phosphorylated. All phosphopeptides were identified with high precision, with a mass tolerance of < 5 ppm for peptide ions (Fig. 1D). The 3575 identified phosphopeptides contained 3918 phosphorylation sites (filtered with site-localization probability > 0.75) and belonged to 1303 phosphoproteins (Table S2). For the identified phosphorylation sites, 3028 (77.3%) were localized on serine (S), 727 (18.6%) on threonine (T)

and only 163 (4.2%) on tyrosine (Y) (Fig. 1E). These results suggested that the distribution of phosphorylation sites of YLT had similar patterns with that of other species, such as porcine muscle (Huang et al., 2014), ovine muscle (Chen et al., 2019b), and human skeletal muscle (Højlund et al., 2009). In addition, 724 of the YLT phosphoproteins carried only one phosphorylation site (55.6%), 228 of them (17.5%) carried two phosphorylation sites, and 351 (26.9%) carried multiple phosphorylation sites (Fig. 1F).

3.3. N-glycoproteome of YLT

A total of 279 N-glycopeptides were identified with high quality (mass error < 5 ppm) (Fig. 1G). These N-glycopeptides were matched to 204 N-glycoproteins, and contained 285 N-glycosites (Table S3). Among the 204 identified YLT N-glycoproteins, 148 (72.5%) carried a single N-glycosite, 41 (20.1%) carried two N-glycosites, and 15 (7.4%) carried multiple N-glycosites (Fig. 1H).

The number of phosphoproteins identified in YLT was 6.38-times that of N-glycoproteins. The number of phosphorylation sites was 13.75-times that of N-glycosites. These ratios were similar to the ratios discovered in the proteomic analysis of Tartary buckwheat seeds (Geng et al., 2019a), but different from those of eggshell matrix and quail eggs, in which there were more N-glycosides than phosphorylation sites (Liu et al., 2020b; Yang et al., 2020). In some proteomic studies on mice, 3803 phosphoproteins and 977 N-glycoproteins were identified from C2C12 myoblasts (Chen et al., 2021), whereas 383 phosphorylated proteins and 544 N-glycoproteins were identified in brain tissue (Zhang et al., 2010). Therefore, there is no conclusive evidence that phosphorylation is more prevalent in animal cells and organ tissues. There are two possible reasons for the quantitative difference between the phosphoproteome and N-glycoproteome of YLT. First, during enrichment, the affinity between IMAC and phosphopeptides was stronger than that between HILIC and glycopeptides. In particular, the diversity of glycopeptides would reduce their specificity and affinity (Geng et al., 2019a) so that phosphopeptides would be enriched more efficiently. The second reason is additional deglycosylation, which increases the loss of glycopeptides before analyses. These technical details need to be considered in future proteomic studies on post-translational modification.

3.4. Phosphorylation and N-glycosylation motifs of YLT

Site-specific patterns of amino acids around a set of phosphorylation sites can be seen from phosphorylation motifs, which provide important information for predicting the kinases upstream of phosphorylation, and the potential function of phosphoproteins. Enriched phosphorylation motifs were identified using Motif-X, and 31 phosphorylation motifs were identified from 2658 phosphorylation sites, including 25 phosphoserine motifs and six phosphothreonine motifs (Fig. S1). The top-10 phosphorylation motifs that matched with the highest number of phosphorylation sites are shown in Fig. 2A. Among them, [sP] and [Rxxs] were the two most common motifs, with 263 and 244 matches, respectively, followed by [Rxxxxxs], [Kxxxxxs], and [Rxs] motifs, all of which matched with > 130 phosphorylation sites. Several other high-frequency motifs (matches > 100) included [RRxs], [sxE], [PxsP] and [RxxsP]. In earlier studies (Chen et al., 2019b; Yang et al., 2020), [sP] and [Rxxs] were also the two most frequent patterns, whereas the frequency of the other patterns varied considerably between species.

Compared with phosphorylation, N-glycosylation motifs are less diverse, with two main conserved types: [NxT] and [NxS] (where "x" is not a proline) (Fig. 2B). In brief, [NxT] matched N-glycosites (145 unique peptides, 50.9%) and [NxS] matched N-glycosites (120 unique peptides, 42.1%) were the most common, with additional N-glycosites matched to some non-conserved motifs (20 peptides, 7.02%). These findings indicated that most of the N-glycosites found in YLT were located on conserved sequences, and that the proportion of low-

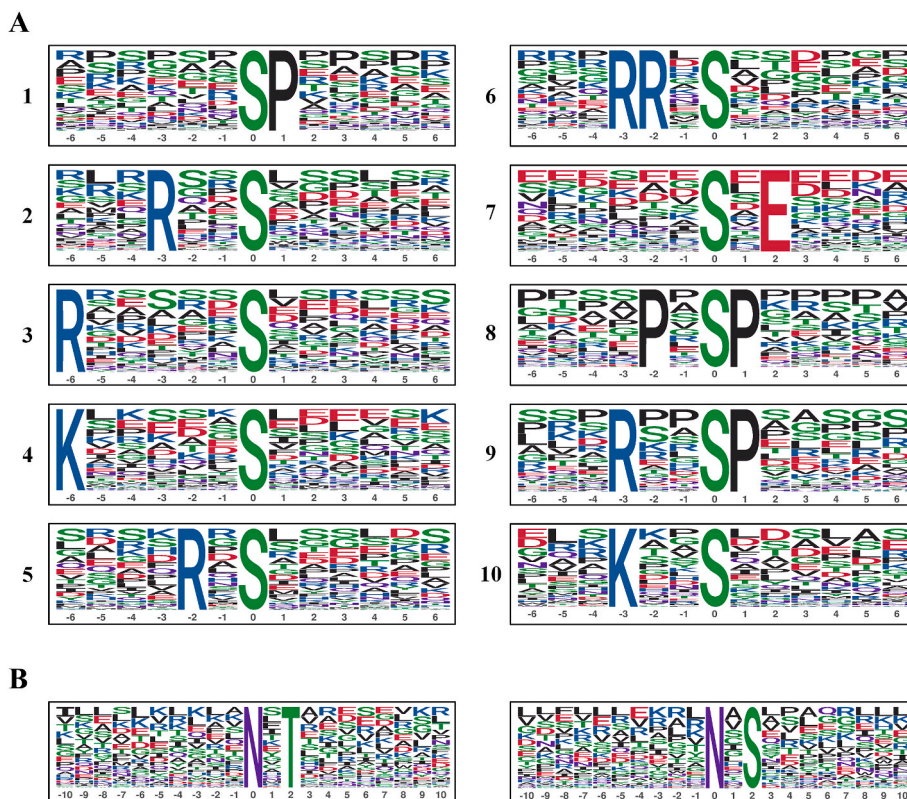


Fig. 2. Significantly enriched phosphorylation motifs (A) and N-glycosylation motifs (B). In the motif names, the lowercase letters “s” and “t” indicate a phosphoserine or phosphothreonine residue at that position, and “x” indicates any amino acid.

frequency non-classical N-glycosylation modifications was small. Notably, more leucine was distributed around [NxT] and [NxS] motifs, with leucine in the [NxT] motif distributed mainly before the N-glycosite, whereas it was distributed evenly before and after in the [NxS] motif. This leucine-rich motif of N-glycoproteins may be involved in protein–protein interactions and, thus, in the immune response.

3.5. “Panorama” of the YLT

A total of 2650 proteins were identified in YLT after merging the common proteome, phosphoproteome, and N-glycoproteome (Fig. 3). Integration of proteome data resulted in a 31.6% increase in the number of YLT proteins compared with the common proteome. This result might be because some low-abundance phosphoproteins and N-glycoproteins were enriched before identification by LC-MS/MS (Geng et al., 2019a). Among the 2649 proteins identified in YLT, 1169 (44.13%) were identified as unmodified, and only 26 (0.98%) were identified as both phosphorylated and N-glycosylated. Details of these dual-modified YLT proteins are summarized in Table S4, and they may have both phosphorylated and N-glycosylated typical functions (Hao et al., 2011). In addition, these results will enrich the YLT protein database.

3.6. Functional annotation of YLT proteins

3.6.1. Subcellular localization of YLT proteins

The subcellular localization of the identified YLT proteins was predicted. For the 1812 common proteins identified in YLT, the cytoplasm (39.8%) was their main localization. Consistent with previous predictions on the subcellular localization of yak *longissimus dorsi* proteins (Zuo et al., 2018). In addition, 79.8% of them were intracellular, 10.5% were extracellular, and 6.0% were localized on the plasma membrane (Fig. 4A). Compared with common proteins, the 1303 phosphoproteins identified in YLT had different localization patterns. The nucleus

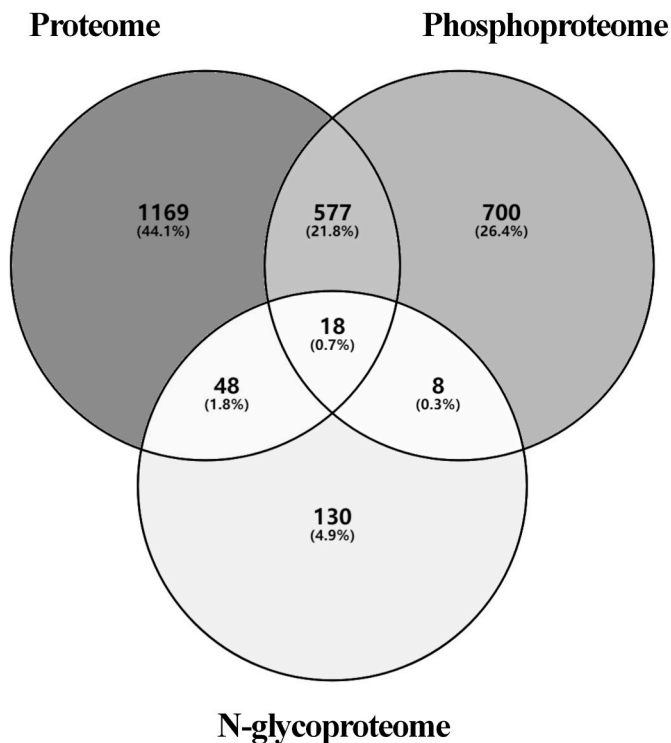


Fig. 3. Overlap of the identified proteomes of yak *longissimus thoracis*.

(43.7%) was the main localization region for phosphoproteins, a smaller proportion (4.1%) of phosphoproteins were located extracellularly, and a larger proportion (8.7%) of phosphoproteins were localized on the

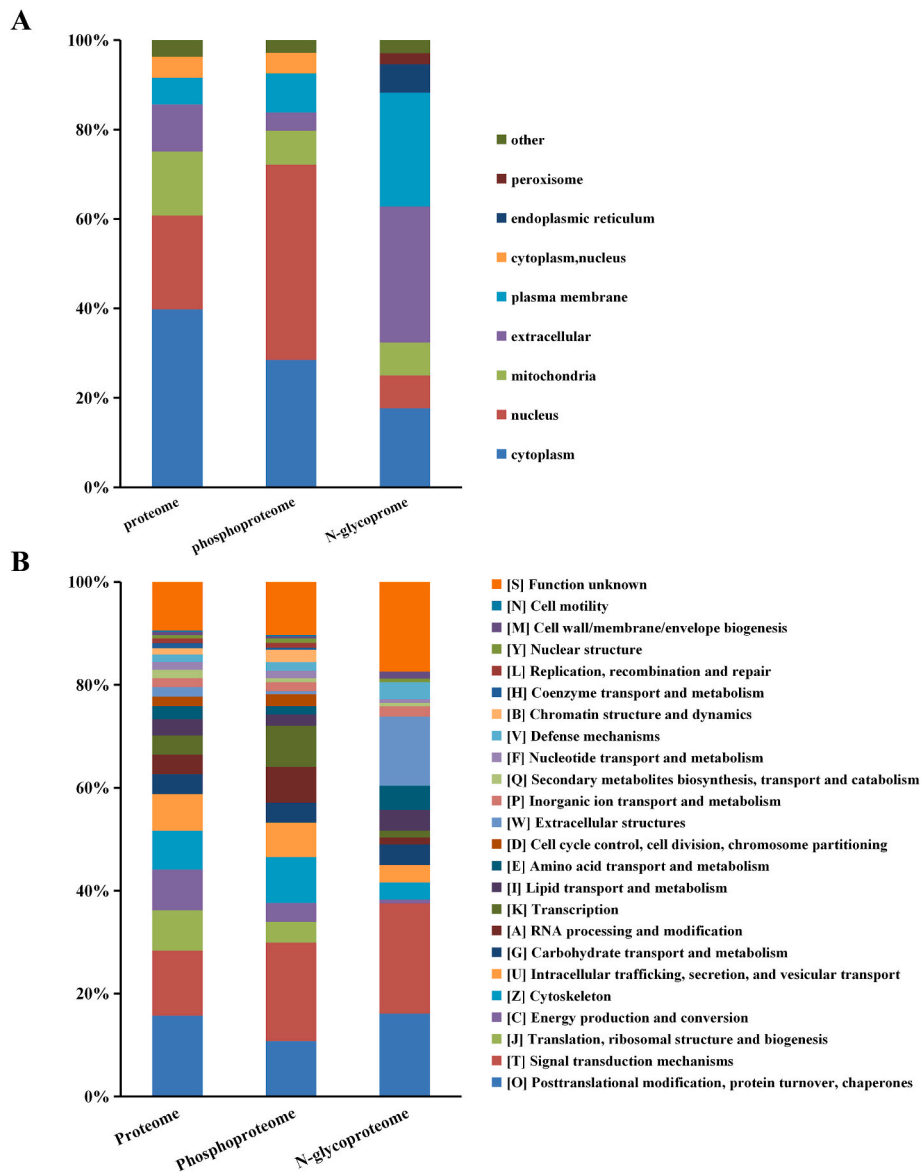


Fig. 4. Predicted subcellular localization and COG/KOG functional classification of identified common proteins, phosphoproteins and glycoproteins. (A), Subcellular localization of common proteins; phosphoproteins; glycoproteins; (B), COG/KOG functional classification of common proteins, phosphoproteins, and glycoproteins.

plasma membrane. The localization of N-glycoproteins in YLT was distinctive: 30.3% of N-glycoproteins were localized extracellularly, 25.5% in the plasma membrane, 6.4% in the endoplasmic reticulum, and 2.5% in peroxisomes.

The distribution of subcellular localization of common proteins, phosphoproteins, and N-glycoproteins in YLT is relevant to post-translational modifications of protein function. Phosphoproteins are involved mainly in physiological processes in the nucleus, such as the phosphorylated histones and transcription factors that regulate gene expression. N-glycoproteins are involved more closely in the physiological processes of cell membranes and the extracellular matrix (ECM) because they need to be processed in the endoplasmic reticulum (Sun and Hood, 2014). Analyses of their subcellular localization showed that the different localizations of common proteins, phosphoproteins, and N-glycoproteins of YLT may be responsible for different physiological functions in muscle.

3.6.2. Eukaryotic orthologous groups (KOG) annotation of YLT proteins

The KOG subcategories with the largest number of common proteins in YLT were [O], [T], [J], [C], [Z], and [U], which were similar to the

KOG classification results of common bovine *longissimus thoracis* proteins (He et al., 2017; Li et al., 2022). These KOG subcategories were involved mainly in protein processing, energy metabolism, cytoskeleton, and material transport, which suggested that the function of common proteins in YLT was centered on muscle activity (Fig. 4B). The KOG classification of YLT phosphoproteins were represented by subcategories of [T], [O], [Z], [U], [K], and [A]. Compared with the common proteins in YLT, a higher proportion of YLT phosphoproteins were involved in signal transduction, transcription, and RNA processing (regulation of gene expression). The annotated KOG subcategories of YLT N-glycoproteins were represented by [T], [O], and [W]. The proportion of N-glycoproteins involving “[W] Extracellular structures” was much higher than that of common proteins and phosphoproteins. In addition, no N-glycoproteins were involved in “[J] Translation, ribosomal structure and biogenesis”, and only one N-glycoproteins was involved in “[C] Energy production and conversion”. Annotation and classification using KOG revealed the functional differences between the common proteins, phosphoproteins, and N-glycoproteins in YLT.

3.6.3. GO annotation of YLT proteins

GO annotation and classification were carried out to further reveal the function of the identified YLT proteins. The common proteins in YLT were classified into nine terms related to binding function and four terms related to catalytic activity under the molecular function (MF) category (Fig. 5A). GO annotation and classification of the YLT phosphoproteins revealed similar results. Differently, YLT N-glycoproteins were involved in four unique GO terms: “amide binding”, “lipid binding”, “signaling receptor activity”, and “transmembrane transporter activity”; and a higher proportion were involved in “macromolecular complex binding”.

In the category of biological processes (BP), the highest number of common proteins in YLT were involved in the GO terms of metabolism (“organic substance metabolic process”, “cellular metabolic process”, “primary metabolic process”), organization (“cellular component organization”, “establishment of localization”, “anatomical structure development”), and stress response (“cellular response to stimulus”, “response to chemical”, “response to stress”) (Fig. 5B). The distribution of phosphoproteins according to GO annotations was similar to that of common proteins but differed in terms of individual GO terms. For instance, 187 phosphoproteins were annotated to “macromolecule localization”, but no phosphoproteins were annotated to “catabolic process”. The GO annotations of YLT N-glycoproteins showed some differences, with three unique GO terms (“anatomical structure morphogenesis”, “cell adhesion”, and “system process”) and three default GO terms (“biosynthetic process”, “cellular component biogenesis”, and “cellular localization”).

In the category of cellular components (CC), the top-three terms with the highest number of common proteins, phosphoproteins, and N-glycoproteins were “intracellular”, “organelles”, and “membrane-bound organelles” (Fig. 5C). The common proteins in YLT involved two unique GO terms: “catalytic complex” and “envelope”. YLT N-glycoproteins were involved in four unique GO terms (“cell surface”, “extracellular space”, “intrinsic component of membrane”, and “whole membrane”) and a much higher proportion were involved in “cell periphery”, “endomembrane system”, and “plasma membrane”. These results suggested a higher involvement of N-glycoproteins in membrane-related functions and extracellular physiological activities (Cao et al., 2017, 2019; Sun and Hood, 2014).

3.7. The common proteins in YLT were involved mainly in myofibril structure and energy metabolism

Enrichment analyses using GO and KEGG databases were carried out using all the protein sets of yaks in the UniPort database as the background. Therefore, the results of enrichment analyses could reveal the major functional or physiological activities that the identified YLT proteomes were involved in.

In the enrichment analyses of the common proteomes in YLT using the GO database, several terms related to the function of muscle contraction were enriched significantly, as represented by “myofibril”, “structural constituent of muscle”, “actin-myosin filament sliding”, and “striated muscle cell differentiation” (Fig. S2). In addition, two KEGG pathways (“focal adhesion” and “tight junction”) associated with the anchorage of muscle fibers, and one KEGG pathway (“cardiac muscle contraction”) associated with muscle-contraction activities were enriched significantly (Fig. 6A, Table S5). These results suggested that the top priority of the common proteins in YLT were involved in the construction of muscle-fiber structure. This finding is consistent with the primary function of muscle tissue. The structure of muscle fibers has a dominant effect on the texture characteristics of meat. For instance, the texture of beef is significantly different from that of pork and lamb because the muscle fibers and muscle bundles have a larger diameter. Furthermore, differences in texture between different types of beef, such as Nelore (*Bos indicus*) and Nelore × *Bos taurus* beef cattle, are evident due to differences in management of breeding and feeding (Curi et al.,

2011). There are large genetic and physiological differences between yak and common commercial breeds of beef cattle (Wang et al., 2016), so differences in muscle fibers and muscle structure should be studied and compared in more detail to deepen understanding of their meat-quality characteristics. Therefore, the common proteins in YLT associated with muscle structure and muscle contraction are important candidate proteins for further study of the quality of yak meat.

Muscle contraction requires a large amount of energy (Fig. 6B). Correspondingly, three representative GO terms related to energy metabolism (“mitochondrion”, “oxidoreductase activity, acting on NAD (PH)”, and “NAD binding”) were enriched significantly. Mitochondria are the main organelles of energy production for the physiological activities of yak muscles. The proteins in the mitochondrial matrix are involved in oxidative phosphorylation, the citric acid cycle, and pyruvate metabolism. Correspondingly, KEGG pathways related to energy metabolism, such as “oxidative phosphorylation”, “TCA cycle”, “glycolysis/gluconeogenesis”, “fatty acid degradation”, and “thermogenesis”, were the most enriched KEGG pathways. In addition, “pyruvate metabolism” and “pentose phosphate pathway”, which are related to substance-transformation pathways, were also enriched. These enriched KEGG pathways with mitochondria as the core not only provide energy but also ensure material transformation to meet the physiological-activity needs of muscle tissue. Related to the regulation of energy metabolism, we discovered “insulin signaling pathway” and “glucagon signaling pathway” to be enriched. Glucose homeostasis must be controlled accurately in muscle tissue because the physiological activities of muscle tissue must ensure a balance between the intake and consumption of glucose.

The involvement of many common proteins in YLT in energy metabolism is closely related to the adaptability of yaks on mountain plateaus. In a comparison of the *longissimus thoracis* proteomes of yak and cattle, Wen and colleagues (Wen et al., 2019) found that proteins related to energy production were more abundant in yak muscle. Results of a quantitative lipidomic analysis between cattle-yak muscles and yak muscles revealed that the higher content of long-chain acylcarnitine in yak muscle might be related to the standby energy supply required for adaptability on mountain plateaus (Gu et al., 2021). In studies on the adaptation to mountain plateaus by yaks, mitochondrial proteins in yak brains were closely related to their highland adaptation (Ma et al., 2021). Therefore, energy metabolism-related pathways are the research focus of adaptation by yaks to mountain plateaus. Energy metabolism dominates the *post mortem* physiological process of meat: rigor mortis and aging. Different types of homeostasis of energy metabolism necessitate different *post mortem* management of yak meat, and the related process parameters must be studied and optimized in detail to avoid abnormal meat quality. The identification and analysis of the proteome of yak muscle would provide important clues for optimization of *post mortem* management.

3.8. YLT phosphoproteins were involved mainly in myofibril organization, regulation of energy metabolism, and signaling

Consistent with the common proteins in YLT, many GO terms related to the structural organization and function of muscle were most significantly enriched by YLT phosphoproteins (Fig. S3). These included “myofibril”, “sarcomere”, “I band”, “supramolecular polymer”, and “Z disc” under the CC category; “structural constituent of muscle”, “actin binding”, “actinin binding”, and “alpha-actinin binding” under the MF category; “muscle filament sliding”, “sarcomere organization”, and “actin-myosin filament sliding” under the biological processes category. Among them, “myofibril” (GO:0030016) was the most representative enriched term with a fold enrichment of 5.92, and was involved in 91 phosphoproteins. Notably, myofibrils and sarcomeres are the contractile units of skeletal muscle cells. Therefore, these results suggested that post-translational phosphorylation was critical for the organization and construction of muscle structures. Phosphorylation can regulate the

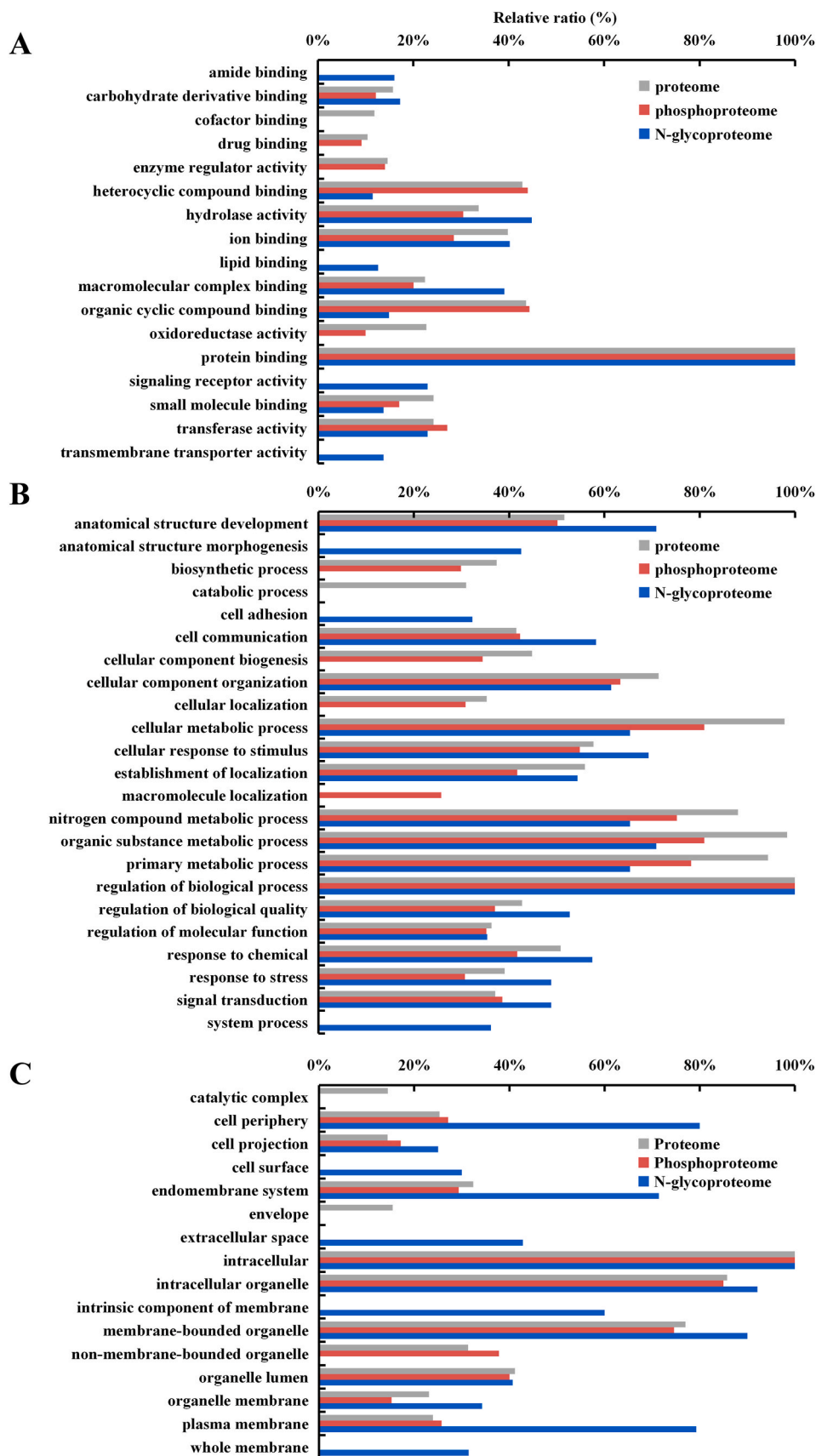
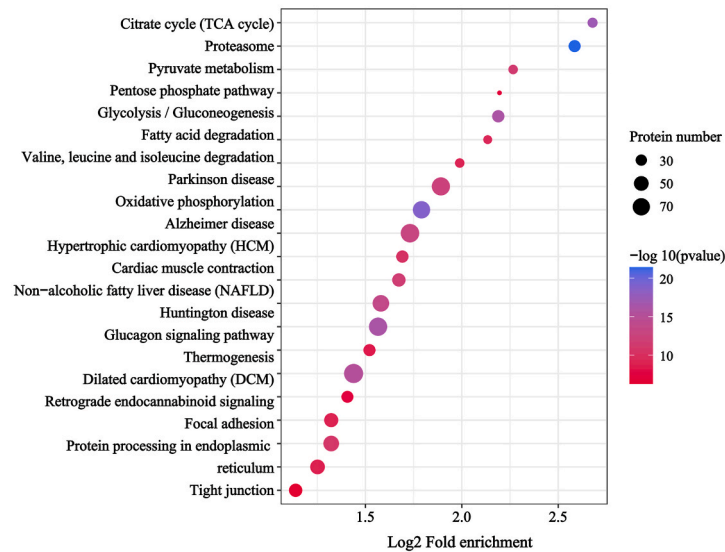


Fig. 5. GO annotated classification of proteins, phosphoproteins, and N-glycoproteins. (A), Biological process; (B), cellular component; (C), molecular function.

A



B

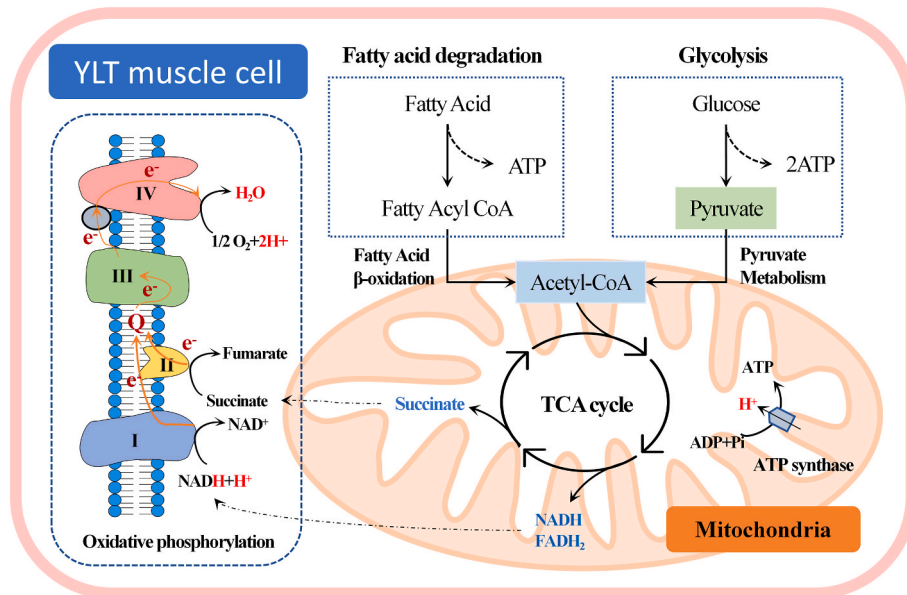


Fig. 6. Enrichment analyses of identified common proteins in yak *longissimus thoracis*. (A), KEGG enrichment result; (B), The 5 most representative enrichment pathways.

interaction between proteins mainly by changing the charge on the surface of proteins which, in turn, affects the organization of myofibrils and sarcomeres. The critical role of phosphorylation in the organization of muscle structure makes it a key regulator of *post mortem* meat quality. For example, it has been reported that dephosphorylation can promote the degradation of myofibrillar proteins by μ -calpain (Li et al., 2017). Phosphorylation levels of sarcomeric proteins have been found to be altered significantly in stress-induced dysfunctional chicken breasts, and these differentially phosphorylated proteins mainly regulated rigor mortis in muscles and were closely related to meat quality (Xing et al., 2017).

YLT phosphoproteins were also involved in energy metabolism. Seven enriched GO terms (GO:0009156, GO:0006090, GO:0046031, GO:0006165, GO:0042866, GO:0046939, and GO:0009135) were closely related to energy metabolism, and represented by “nucleoside diphosphate phosphorylation” (with 19 YLT phosphoproteins and a fold enrichment of 4.97) and “pyruvate metabolic process” (with 25 YLT phosphoproteins and a fold enrichment of 4.63). In the enrichment

analyses of YLT phosphoproteins using the KEGG database, “pyruvate metabolism” (map00620) and “glycolysis/gluconeogenesis” (map00010) were among the most enriched pathways (Fig. 7A). The YLT phosphoproteins involved in pyruvate metabolism merit special attention because pyruvate metabolism is the key process linking glycolysis and the citric acid cycle, and is also an important node in the transformation of nutrients (amino acids, monosaccharides, and fatty acids). Substance turnover in yak muscle needs to be more flexible and regulated carefully in response to high-altitude environments. This might imply that the phosphorylation levels of enzymes related to “pyruvate metabolism” are different compared with those in plain cattle, which needs to be compared quantitatively in future studies.

YLT phosphoproteins played a more important part in signaling besides regulating the organization of myofibrils and the activity of enzymes related to energy metabolism. Ten of the top-25 enriched KEGG pathways were related to signaling (Fig. 7B). Among them, “insulin signaling pathway” (map04910), “glucagon signaling pathway” (map04922), and “AMPK signaling pathway” (map04152) are

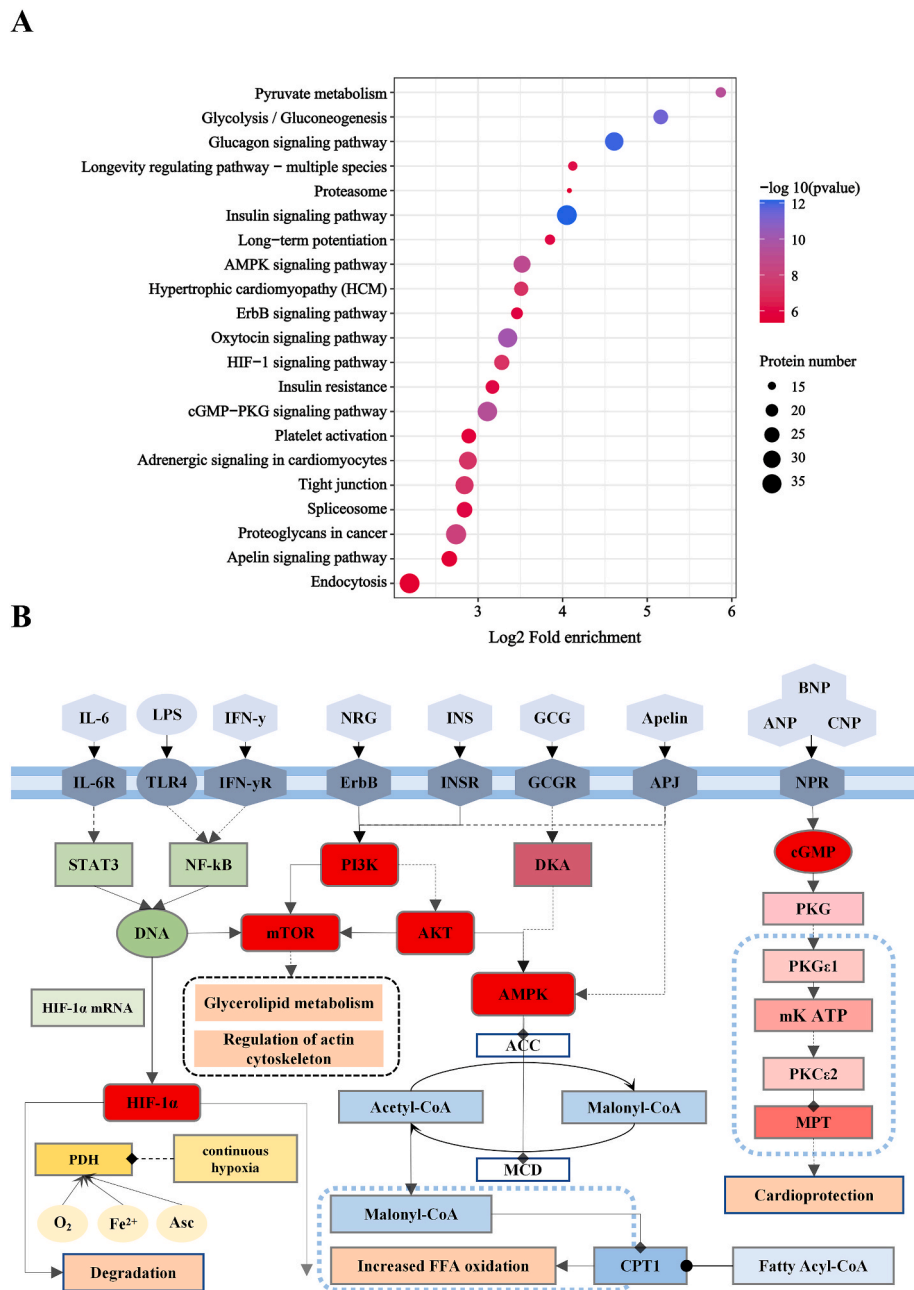


Fig. 7. Enrichment analyses of identified phosphoproteins in yak *longissimus thoracis*. (A), KEGG enrichment result; (B), Enrichment pathways of phosphoproteins involved in signaling.

responsible for the homeostatic regulation of energy metabolism; the “HIF-1 signaling pathway” (map04066) is responsible for intracellular sensing and regulation of hypoxia. These enriched signaling pathways are “sensors” of oxygen and energy status in cells and tissues, and “direct” cells to respond, thereby ensuring well-executed and sustained muscle contractions. It has been reported that hypoxia-inducible factor (HIF)-1 α can regulate nucleotide metabolism in the ischemic heart to reduce adenosine accumulation and protect cardiac function (Wu et al., 2015). In addition to signaling of the intracellular environment and energy homeostasis, muscles must remain responsive to cytokines and second messengers. The enriched “ErbB signaling pathway” (map04012) and “apelin signaling pathway” (map04371) are responsible for cytokine (first messenger) sensing and signal transduction; “cGMP-PKG signaling pathway” (map04022) and “mTOR signaling pathway” (map04150) are important second-messenger signaling pathways. These signaling pathways are involved in regulation of a wide

range of cellular physiological activities to coordinate the rapid response of myofibrils in muscle contraction. Most of the YLT phosphoproteins involved in the signaling pathways stated above are kinases. Correspondingly, in the enrichment analyses using the GO database, the significantly enriched term “kinase binding” involved 98 YLT phosphoproteins. These kinases and their phosphorylation sites identified in this work provide important information for investigation of the signaling-regulatory mechanisms in yak muscle.

Phosphorylation of muscle proteins has a key role in post-slaughter physiology due to its critical signaling and regulatory functions. First, phosphorylation regulates *post mortem* energy metabolism in muscle and, thus, affects muscle pH. Anderson and colleagues showed phosphorylation of phosphoglucomutase 1 to be closely associated with post-slaughter beef tenderness (Anderson et al., 2014). In detail, the phosphoglucomutase 1 phosphorylated in beef early after slaughter accelerates the rate of pH decline, leading to greater final muscle segment

length (Silva et al., 2019). When the pH in muscle is reduced close to the isoelectric point of protein, the water-holding capacity of longissimus lumbosus muscle of yak decreases (Zuo et al., 2016), whereas pale soft exudative meat occurs in pork (Xu et al., 2021). In addition, two groups of proteins with different levels of phosphorylation in goat muscle (PFK, MYL2 and HSP27) regulate muscle stiffness, which leads to muscle conversion to high- or low-quality meat (Liu et al., 2018). Second, the phosphorylation of proteolytic enzymes and their upstream regulators can affect their activity and stability, thereby regulating the hydrolysis of myofibrils and muscle tissue. It has been reported that phosphorylation and dephosphorylation of μ -calpain changes its secondary structure which, in turn affects its activity and autolysis (Du et al., 2018). Due to the critical role of μ -calpain in Z-disk disintegration, the changes induced by its phosphorylation would have an important impact on meat tenderness. Electrical stimulation accelerated the tenderization of meat after slaughter, while dephosphorylation enhanced the precise degradation of myogenic fibronectin by μ -calpain (Li et al., 2012, 2017). In addition, phosphorylation of myosin regulatory light chain at Ser17 could improve actin–myosin binding and interactions, which may improve meat quality (Cao et al., 2021).

3.9. YLT N-glycoproteins were involved mainly in cellular immunity, organismal homeostasis, and extracellular matrix (ECM) organization

Unlike the common proteins and phosphoproteins in YLT, which are involved mainly in myofibril construction, N-glycoproteins in YLT participate mainly in ECM organization. In the enrichment analyses of YLT N-glycoproteins using the GO database, terms such as “extracellular matrix”, “integrin binding”, “laminin binding”, and “collagen binding” were enriched significantly (Fig. S4). Correspondingly, “ECM-Receptor Interaction” (map04512), “focal adhesion” (map04510), and “Cell adhesion molecules (CAMs)” (map04514) were enriched in the enrichment analyses of YLT N-glycoproteins using the KEGG database (Fig. 8A). The most representative YLT N-glycoproteins involved in these pathways and terms were six types of laminins (20 N-glycosites), five kinds of integrins (eight N-glycosites), and three types of collagens (six N-glycosites). These ECM N-glycoproteins have important roles in myofibril organization and muscle contraction (Fig. 8B). N-glycosylation modifications can affect the binding capacity of laminin and may also promote the development and differentiation of muscle cells (Cabrera et al., 2012). In a recent study, β 1 and α 2 integrins were

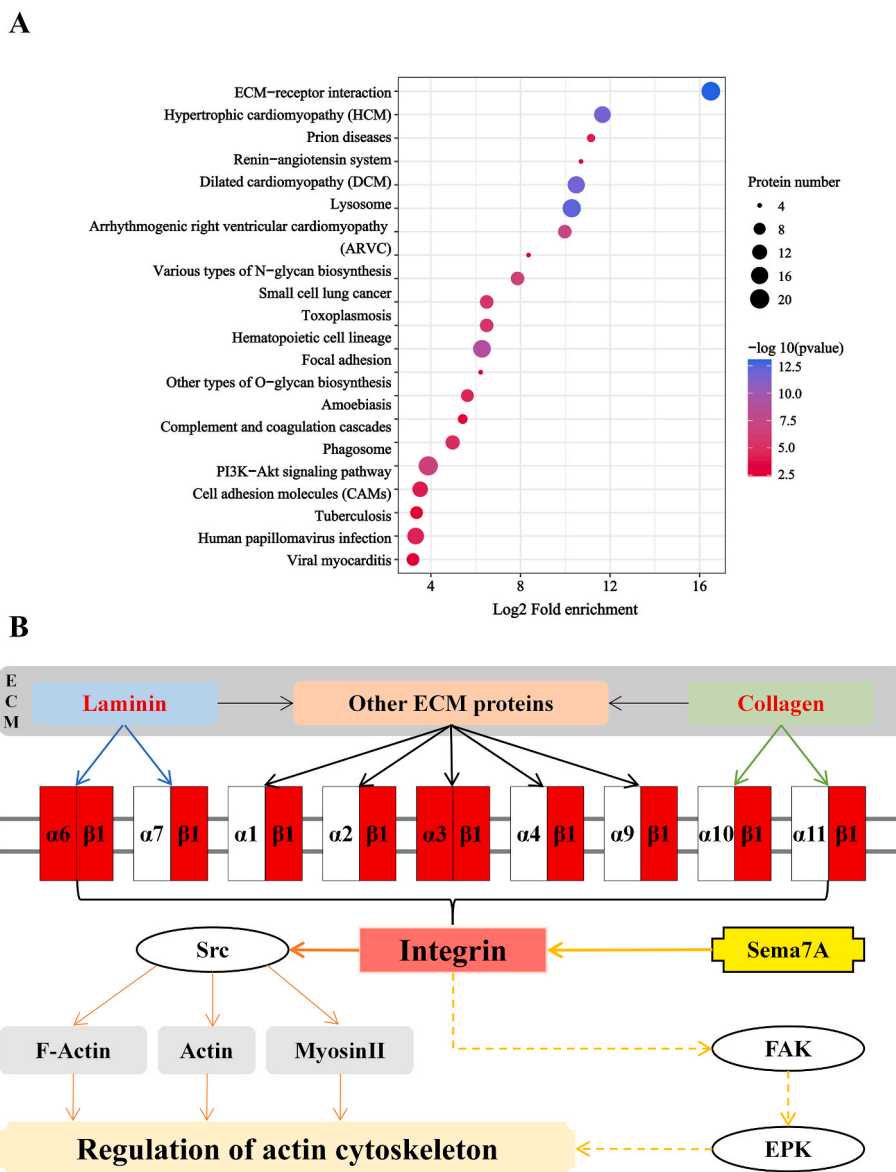


Fig. 8. Enrichment analyses of identified N-glycoproteins in yak *longissimus thoracis*. (A), KEGG enrichment result; (B), Functions of 3 N-glycoproteins in the “ECM-Receptor Interaction”.

isolated from megakaryocytes of Vav1-hJAK2^{V617F} mice and control mice. Glycosylation of both types of integrins affected Janus kinase-2 activity, which induced myelofibrosis in mice (Gaye et al., 2022). In addition, glycosylation of type-IV collagen regulates binding of $\alpha 2\beta 1$ and $\alpha 3\beta 1$ integrin in melanocytes (Stawikowski et al., 2014), and remodels the ECM (Jürgensen et al., 2011) which, in turn, improves muscle tenderness. Those studies suggest that N-glycosylation is critical for the function of ECM proteins. Although N-glycoproteins have been studied less in livestock-produced meat, there is a need to study the role of N-glycosylation of ECM proteins (especially collagen) in *post mortem* muscle physiology and meat quality due to their importance in meat tenderness.

In the present study, YLT N-glycoproteins had an important role in the ECM but also participated in the immune response, acting in inflammation elimination during the growth and development of muscle cells. Notably, “phagosome” (map04145) and “complement and coagulation cascades” (map04610) pathways were enriched in the enrichment analyses of YLT N-glycoproteins using the KEGG database, and these pathways were closely associated with immunity. The most representative N-glycoproteins involved in the “phagosome” pathway were integrin β , lysosome-associated membrane glycoproteins, and the immunoglobulin epsilon chain C region. Antibodies that interfere with integrin–ligand binding inhibit cell migration *in vitro* and reduce tumor growth *in vivo* (Engebraaten et al., 2009; Janik et al., 2010). Glycosylation modifications of integrins could interfere with some types of glycoprotein-mediated cell adhesion and promote dissociation of tumor cells. Lysosome-associated membrane glycoproteins are a class of highly glycosylated proteins whose overexpression promotes the adhesion and invasion of cancer cells (Nishino et al., 2022; Wang et al., 2017). Also, the N-glycoproteins lysosomal associated membrane proteins (LAMP 1 and LAMP 2) are involved in myotube formation (Sakane and Akasaki, 2018), and affect post-slaughter meat quality. Immunoglobulins have immunomodulatory and anti-inflammatory effects, and the biological activity of immunoglobulin-G is regulated by Fc N-glycosylation, which is associated with various inflammatory diseases (Selman et al., 2011). In addition, three complement-associated N-glycoproteins (L8IXQ0, L8IN50 and L8HZV8) and three coagulation-associated N-glycoproteins (L8IMX1, L8I117 and L8IH10) were included in the “complement and coagulation cascade”. The complement system (as an important part of the innate immune system) can form adaptive immunity by lysing pathogens directly. Complement and coagulation are closely related and work together to protect an organism from injury (Oikononopoulou et al., 2012). In conclusion, these identified YLT N-glycoproteins were involved in regulating inflammation and the immune response, which would make yaks more resistant to diseases under the harsh environment of extreme cold and low oxygen. These results would provide some reference value for research on N-glycoproteins in livestock animals.

In addition, YLT N-glycoproteins have a role in regulating homeostasis in the body. In the enrichment analyses of YLT N-glycoproteins using the GO database, “regulation of metal ion transport” (GO:0010959) and “inorganic ion homeostasis” (GO:0098771) related to ion transport regulated homeostasis of the cellular microenvironment of the body; “platelet degranulation” (GO:0002576) and “regulation of wound healing” (GO:0061041) were associated with tissue repair and were involved in the healing, growth, and proliferation of cells. Among them, triadin is an important class of protein for the maintenance of skeletal-muscle function (Oddoux et al., 2009), and angiotensin-converting enzyme plays a part in blood-pressure regulation and vascular remodeling (Kost et al., 2018). Besides, being present in a digestive organ, a “lysosome” (map04142) contains various hydrolytic enzymes and its surface is highly glycosylated. A lysosome releases acidic hydrolases to digest pathogenic bacteria and other substances and protects itself from digestion, but also has an autonomous metabolic function. In summary, the N-glycoproteins in YLT had muscle-remodeling functions, but also had prominent roles in healing of the immune system and homeostasis regulation. These functions may be

linked inextricably to the growing environment of yaks. In particular, their relationship with adaptation to mountain plateaus merits further study.

4. Conclusions

This was the first investigation of the integrated common proteome, phosphoproteome, and N-glycoproteome of YLT. Based on offline high-pH RPLC separation, phosphopeptides/glycopeptides enrichment, and LC-MS/MS identification, 1812 common proteins, 1303 phosphoproteins, and 204 N-glycoproteins were identified. Analyses of pathway enrichment using GO and KEGG databases revealed that the common proteins in YLT were involved mainly in myofibril structure and energy metabolism, YLT phosphoproteins were involved mainly in myofibril organization, regulation of energy metabolism, and signaling, and YLT N-glycoproteins were involved mainly in ECM organization, cellular immunity, and organismal homeostasis. These results suggest that the identified YLT proteins have important roles in the post-mortem physiology of yak beef. The information in this study can aid exploration of the quality characteristics of yak beef.

CRedit authorship contribution statement

Xinping Chang: Investigation, Data curation, Writing – original draft. **Jiamin Zhang:** Resources, Writing – review & editing. **Zhendong Liu:** Resources, Data curation. **Zhang Luo:** Funding acquisition, Writing – review & editing. **Lin Chen:** Resources, Data curation. **Jinqiu Wang:** Project administration, Methodology. **Fang Geng:** Writing – original draft, Writing – review & editing, Supervision.

Declaration of competing interest

The authors declare that they have no known competing financial interests or personal relationships that could have appeared to influence the work reported in this paper.

Acknowledgments

This work was supported by the Central Support Special Fund for the Reform and Development of Tibet Local Colleges and Universities (KY2022ZY-03), National Natural Science Foundation of China (31860425).

Appendix A. Supplementary data

Supplementary data to this article can be found online at <https://doi.org/10.1016/j.crfs.2022.09.012>.

References

- Anderson, M.J., Lonergan, S.M., Lonergan, E., Huff, 2014. Differences in phosphorylation of phosphoglucosylase 1 in beef steaks from the longissimus dorsi with high or low star probe values. *Meat Sci.* 96 (1), 379–384. <https://doi.org/10.1016/j.meatsci.2013.07.017>.
- Antonelo, D.S., Gómez, J.F.M., Silva, S.L., Beline, M., Zhang, X., Wang, Y., Pavan, B., Koulicoff, L.A., Rosa, A.F., Goulart, R.S., Li, S., Gerrard, D.E., Suman, S.P., Wes Schilling, M., Balieiro, J.C.C., 2022. Proteome basis for the biological variations in color and tenderness of longissimus thoracis muscle from beef cattle differing in growth rate and feeding regime. *Food Res. Int.* 153, 110947 <https://doi.org/10.1016/j.foodres.2022.110947>.
- Cabrera, P.V., Pang, M., Marshall, J.L., Kung, R., Nelson, S.F., Stalnak, S.H., Wells, L., Crosbie-Watson, R.H., Baum, L.G., 2012. High throughput screening for compounds that alter muscle cell glycosylation identifies new role for N-glycans in regulating sarcolemmal protein abundance and laminin binding. *J. Biol. Chem.* 287 (27), 22759–22770. <https://doi.org/10.1074/jbc.M111.334581>.
- Cao, C., Xiao, Z., Ge, C., Wu, Y., 2022. Application and research progress of proteomics in chicken meat quality and identification: a review. *Food Rev. Int.* 38 (3), 313–334. <https://doi.org/10.1080/87559129.2020.1733594>.
- Cao, L., Wang, Z., Zhang, D., Li, X., Hou, C., Ren, C., 2021. Phosphorylation of myosin regulatory light chain at Ser17 regulates actomyosin dissociation. *Food Chem.* 356, 129655 <https://doi.org/10.1016/j.foodchem.2021.129655>.

- Cao, X., Song, D., Yang, M., Yang, N., Ye, Q., Tao, D., Liu, B., Wu, R., Yue, X., 2017. Comparative analysis of whey N-glycoproteins in human colostrum and mature milk using quantitative glycoproteomics. *J. Agric. Food Chem.* 65 (47), 10360–10367. <https://doi.org/10.1021/acs.jafc.7b04381>.
- Cao, X., Zheng, Y., Wu, S., Yang, N., Wu, J., Liu, B., Ye, W., Yang, M., Yue, X., 2019. Characterization and comparison of milk fat globule membrane N-glycoproteomes from human and bovine colostrum and mature milk. *Food Funct.* 10 (8), 5046–5058. <https://doi.org/10.1039/C9FO00686A>.
- Chen, L., Bai, Y., Everaert, N., Li, X., Tian, G., Hou, C., Zhang, D., 2019a. Effects of protein phosphorylation on glycolysis through the regulation of enzyme activity in ovine muscle. *Food Chem.* 293, 537–544. <https://doi.org/10.1016/j.foodchem.2019.05.011>.
- Chen, L., Li, Z., Everaert, N., Lametsch, R., Zhang, D., 2019b. Quantitative phosphoproteomic analysis of ovine muscle with different postmortem glycolytic rates. *Food Chem.* 280, 203–209. <https://doi.org/10.1016/j.foodchem.2018.12.056>.
- Chen, L., Li, Z., Li, X., Chen, J., Everaert, N., Zhang, D., 2018. The effect of sarcoplasmic protein phosphorylation on glycolysis in postmortem ovine muscle. *Int. J. Food Sci. Technol.* 53 (12), 2714–2722. <https://doi.org/10.1111/ijfs.13882>.
- Chen, X., Sun, Y., Zhang, T., Roepstorff, P., Yang, F., 2021. Comprehensive analysis of the proteome and PTMomes of C2C12 myoblasts reveals that sialylation plays a role in the differentiation of skeletal muscle cells. *J. Proteome Res.* 20 (1), 222–235. <https://doi.org/10.1021/acs.jproteome.0c00353>.
- Curi, R.A., Chardulo, L.A.L., Arrigoni, M.D.B., Silveira, A.C., de Oliveira, H.N., 2011. Associations between LEP, DGAT1 and FABP4 gene polymorphisms and carcass and meat traits in Nelore and crossbred beef cattle. *Livest. Sci.* 135 (2), 244–250. <https://doi.org/10.1016/j.livsci.2010.07.013>.
- Du, M., Li, X., Li, Z., Shen, Q., Wang, Y., Li, G., Zhang, D., 2018. Phosphorylation regulated by protein kinase A and alkaline phosphatase play positive roles in μ -calpain activity. *Food Chem.* 252, 33–39. <https://doi.org/10.1016/j.foodchem.2018.01.103>.
- Engelbraaten, O., Trikha, M., Juell, S., Garman-Vik, S., Fodstad, Ø., 2009. Inhibition of in vivo tumour growth by the blocking of host $\alpha v\beta 3$ and $\alpha IIb\beta 3$ integrins. *Anticancer Res.* 29 (1), 131–137.
- Gaye, M.M., Ward, C.M., Piasecki, A.J., Stahl, V.L., Karagianni, A., Costello, C.E., Ravid, K., 2022. Characterization of glycoproteoforms of integrins $\alpha 2$ and $\beta 1$ in megakaryocytes in the occurrence of JAK2V617F mutation-induced primary myelofibrosis. *Mol. Cell. Proteomics* 21 (4), 100213. <https://doi.org/10.1016/j.mcp.2022.100213>.
- Geng, F., Liu, X., Wang, J., He, R., Zhao, J., Xiang, D., Zou, L., Peng, L., Zhao, G., 2019a. In-depth mapping of the seed phosphoproteome and N-glycoproteome of Tartary buckwheat (*Fagopyrum tataricum*) using off-line high pH RPLC fractionation and nLC-MS/MS. *Int. J. Biol. Macromol.* 137, 688–696. <https://doi.org/10.1016/j.ijbiomac.2019.07.026>.
- Geng, F., Wang, J.Q., Liu, D.Y., Jin, Y.G., Ma, M.H., 2017. Identification of N-Glycosites in chicken egg white proteins using an omics strategy. *J. Agric. Food Chem.* 65 (26), 5357–5364. <https://doi.org/10.1021/acs.jafc.7b01706>.
- Geng, F., Xie, Y., Wang, J., Li, S., Jin, Y., Ma, M., 2019b. Large-scale purification of ovalbumin using polyethylene glycol precipitation and isoelectric precipitation. *Ovalbumin Sci.* 98 (3), 1545–1550. <https://doi.org/10.3382/ps/pey402>.
- Geng, F., Xie, Y.X., Wang, J.Q., Majumder, K., Qiu, N., Ma, M.H., 2018. N-glycoproteomic analysis of chicken egg yolk. *J. Agric. Food Chem.* 66 (43), 11510–11516. <https://doi.org/10.1021/acs.jafc.8b04492>.
- Gu, X., Gao, Y., Luo, Z., Yang, L., Chi, F., Xiao, J., Wang, W., Geng, F., 2019. In-depth mapping of the proteome of Tibetan pig tenderloin (*longissimus dorsi*) using off-line high-pH reversed-phase fractionation and LC-MS/MS. *J. Food Biochem.* 43 (11), e13015. <https://doi.org/10.1111/jfbc.13015>.
- Gu, X., Sun, W., Yi, K., Yang, L., Chi, F., Luo, Z., Wang, J., Zhang, J., Wang, W., Yang, T., Geng, F., 2021. Comparison of muscle lipidomes between cattle-yak, yak, and cattle using UPLC-MS/MS. *J. Food Compos. Anal.* 103, 104113. <https://doi.org/10.1016/j.jfca.2021.104113>.
- Hao, P., Guo, T., Sze, S.K., 2011. Simultaneous analysis of proteome, phospho- and glycoproteome of rat kidney tissue with electrostatic repulsion hydrophilic interaction chromatography. *PLoS One* 6 (2), e16884. <https://doi.org/10.1371/journal.pone.0016884>.
- He, H., Chen, S., Liang, W., Liu, X., 2017. Genome-wide proteomics analysis on longissimus muscles in Qinchuan beef cattle. *Anim. Genet.* 48 (2), 131–140. <https://doi.org/10.1111/age.12508>.
- Højlund, K., Bowen, B.P., Hwang, H., Flynn, C.R., Madiredy, L., Geetha, T., Langlais, P., Meyer, C., Mandarino, L.J., Yi, Z., 2009. In vivo phosphoproteome of human skeletal muscle revealed by phosphopeptide enrichment and HPLC-ESI-MS/MS. *J. Proteome Res.* 8 (11), 4954–4965. <https://doi.org/10.1021/pr9007267>.
- Huang, H., Larsen, M.R., Palmisano, G., Dai, J., Lametsch, R., 2014. Quantitative phosphoproteomic analysis of porcine muscle within 24 h postmortem. *J. Proteomics* 106, 125–139. <https://doi.org/10.1016/j.jprot.2014.04.020>.
- Janik, M.E., Lityńska, A., Vereecken, P., 2010. Cell migration—the role of integrin glycosylation. *Biochim. Biophys. Acta Gen. Subj.* 1800 (6), 545–555. <https://doi.org/10.1016/j.bbagen.2010.03.013>.
- Jürgensen, H.J., Madsen, D.H., Ingvarsen, S., Melander, M.C., Gårdsvoll, H., Patthy, L., Engelholm, L.H., Behrendt, N., 2011. A novel functional role of collagen glycosylation: INTERACTION with the endocytic collagen receptor uPARAP/ENDO180. *J. Biol. Chem.* 286 (37), 32736–32748. <https://doi.org/10.1074/jbc.M111.266692>.
- Kemp, C.M., Parr, T., 2012. Advances in apoptotic mediated proteolysis in meat tenderisation. *Meat Sci.* 92 (3), 252–259. <https://doi.org/10.1016/j.meatsci.2012.03.013>.
- Kost, O.A., Tikhomirova, V.E., Kryukova, O.V., Gusakov, A.V., Bulaeva, N.I., Evdokimov, V.V., Golukhova, E.Z., Danilov, S.M., 2018. Conformational “fingerprint” of the angiotensin-converting enzyme. *Russ. J. Bioorg. Chem.* 44 (1), 52–63. <https://doi.org/10.1134/S1068162018010107>.
- Li, C.B., Li, J., Zhou, G.H., Lametsch, R., Ertbjerg, P., Brüggemann, D.A., Huang, H.G., Karlsson, A.H., Hviiid, M., Lundström, K., 2012. Electrical stimulation affects metabolic enzyme phosphorylation, protease activation, and meat tenderization in beef. *J. Anim. Sci.* 90 (5), 1638–1649. <https://doi.org/10.2527/jas.2011-4514>.
- Li, X., Qian, S., Huang, F., Li, K., Song, Y., Liu, J., Guo, Y., Zhang, C., Blecker, C., 2022. The investigation of protein profile and meat quality in bovine longissimus thoracic frozen under different temperatures by data-independent acquisition (DIA) strategy. *Foods* 11 (12), 1791. <https://doi.org/10.3390/foods11121791>.
- Li, Z., Li, X., Gao, X., Shen, Q.W., Du, M., Zhang, D., 2017. Phosphorylation prevents in vitro myofibrillar proteins degradation by μ -calpain. *Food Chem.* 218, 455–462. <https://doi.org/10.1016/j.foodchem.2016.09.048>.
- Liu, L., Yang, R., Luo, X., Dong, K., Huang, X., Song, H., Gao, H., Li, S., Huang, Q., 2020. Omics analysis of holoproteins and modified proteins of quail egg. *Food Chem.* 326, 126983. <https://doi.org/10.1016/j.foodchem.2020.126983>.
- Liu, M., Wei, Y., Li, X., Quek, S.Y., Zhao, J., Zhong, H., Zhang, D., Liu, Y., 2018. Quantitative phosphoproteomic analysis of caprine muscle with high and low meat quality. *Meat Sci.* 141, 103–111. <https://doi.org/10.1016/j.meatsci.2018.01.001>.
- Liu, X., Wang, J., Liu, L., Cheng, L., Huang, Q., Wu, D., Peng, L., Shi, X., Li, S., Geng, F., 2021. Quantitative N-glycoproteomic analyses provide insights into the effects of thermal processes on egg white functional properties. *Food Chem.* 342, 128252. <https://doi.org/10.1016/j.foodchem.2020.128252>.
- Liu, X., Wang, J.Q., Huang, Q., Cheng, L., Gan, R., Liu, L.L., Wu, D., Li, H.M., Peng, L.X., Geng, F., 2020. Underlying mechanism for the differences in heat-induced gel properties between thick egg whites and thin egg whites: gel properties, structure and quantitative proteome analysis. *Food Hydrocolloids* 106, 105873. <https://doi.org/10.1016/j.foodhyd.2020.105873>.
- López-Pedrouso, M., Lorenzo, J.M., Di Stasio, L., Brugiapaglia, A., Franco, D., 2021. Quantitative proteomic analysis of beef tenderness of Piemontese young bulls by SWATH-MS. *Food Chem.* 356, 129711. <https://doi.org/10.1016/j.foodchem.2021.129711>.
- Ma, X., Zhang, Q., La, Y., Fu, D., Jiang, H., Bao, P., Wu, X., Chu, M., Guo, X., Yan, P., Liang, C., 2021. Differential abundance of brain mitochondrial proteins in yak and cattle: a proteomics-based study. *Front. Vet. Sci.* 8. <https://www.frontiersin.org/article/10.3389/fvets.2021.663031>.
- Nishino, K., Nishiko, Y., Shibata, M., Oda, Y., Watanabe, E., Niimi, K., Yamamoto, E., Kajiyama, H., 2022. Cell surface membrane lysosome-associated membrane glycoprotein 2 promotes cell adhesion via abundant N-glycans in choriocarcinoma. *Placenta* 117, 109–117. <https://doi.org/10.1016/j.placenta.2021.11.005>.
- Oddoux, S., Brocard, J., Schweitzer, A., Szentesi, P., Giannesini, B., Brocard, J., Fauré, J., Pernet-Gallay, K., Bendahan, D., Lunardi, J., Csernoch, L., Marty, I., 2009. Triadin deletion induces impaired skeletal muscle function. *J. Biol. Chem.* 284 (50), 34918. <https://doi.org/10.1074/jbc.M109.022442>.
- Oikonomopoulou, K., Ricklin, D., Ward, P.A., Lambris, J.D., 2012. Interactions between coagulation and complement—their role in inflammation. *Semin. Immunopathol.* 34 (1), 151–165. <https://doi.org/10.1007/s00281-011-0280-x>.
- Sakane, H., Akasaki, K., 2018. The major lysosomal membrane proteins LAMP-1 and LAMP-2 participate in differentiation of C2C12 myoblasts. *Biol. Pharm. Bull.* 41 (8), 1186–1193. <https://doi.org/10.1248/bpb.b17-01030>.
- Selman, M.H.J., Niks, E.H., Titulaer, M.J., Verschuren, J.J.G.M., Wuhrer, M., Deelder, A.M., 2011. IgG Fc N-glycosylation changes in Lambert-Eaton myasthenic syndrome and myasthenia gravis. *J. Proteome Res.* 10 (1), 143–152. <https://doi.org/10.1021/pr1004373>.
- Silva, L.H.P., Rodrigues, R.T.S., Assis, D.E.F., Benedetti, P.D.B., Duarte, M.S., Chizzotti, M.L., 2019. Explaining meat quality of bulls and steers by differential proteome and phosphoproteome analysis of skeletal muscle. *J. Proteomics* 199, 51–66. <https://doi.org/10.1016/j.jprot.2019.03.004>.
- Stawikowski, M.J., Aukszi, B., Stawikowska, R., Cudic, M., Fields, G.B., 2014. Glycosylation modulates melanoma cell $\alpha 2\beta 1$ and $\alpha 3\beta 1$ integrin interactions with type IV collagen. *J. Biol. Chem.* 289 (31), 21591–21604. <https://doi.org/10.1074/jbc.M114.572073>.
- Sun, B., Hood, L., 2014. Protein-centric N-glycoproteomics analysis of membrane and plasma membrane proteins. *J. Proteome Res.* 13 (6), 2705–2714. <https://doi.org/10.1021/pr500187g>.
- Wang, H.B., Zan, L.S., Zhang, Y.Y., 2014. Profiling of the yak skeletal muscle tissue gene expression and comparison with the domestic cattle by genome array. *Animal* 8 (1), 28–35. <https://doi.org/10.1017/S1757173113001948>.
- Wang, H.C., Shi, F.Y., Hou, M.J., Fu, X.Y., Long, R.J., 2016. Cloning of oligopeptide transport carrier PepT1 and comparative analysis of PepT1 messenger ribonucleic acid expression in response to dietary nitrogen levels in yak (*Bos grunniens*) and indigenous cattle (*Bos taurus*) on the Qinghai-Tibetan plateau. *J. Anim. Sci.* 94 (8), 3431–3440. <https://doi.org/10.2527/jas.2016-0501>.
- Wang, H., Long, R., Liang, J.B., Guo, X., Ding, L., Shang, Z., 2011. Comparison of nitrogen metabolism in yak (*Bos grunniens*) and indigenous cattle (*Bos taurus*) on the Qinghai-Tibetan plateau. *Asian-Australas. J. Anim. Sci.* 24 (6), 766–773. <https://doi.org/10.5713/ajas.2011.10350>.
- Wang, J., Xiao, J., Geng, F., Li, X., Yu, J., Zhang, Y., Chen, Y., Liu, D., 2019. Metabolic and proteomic analysis of morel fruiting body (*Morchella importuna*). *J. Food Compos. Anal.* 76, 51–57. <https://doi.org/10.1016/j.jfca.2018.12.006>.
- Wang, Q., Yao, J., Jin, Q., Wang, X., Zhu, H., Huang, F., Wang, W., Qiang, J., Ni, Q., 2017. LAMP1 expression is associated with poor prognosis in breast cancer. *Oncol. Lett.* 14 (4), 4729–4735. <https://doi.org/10.3892/ol.2017.6757>.

- Wang, Y., Tian, X., Liu, X., Xing, J., Guo, C., Du, Y., Zhang, H., Wang, W., 2022. Focusing on intramuscular connective tissue: effect of cooking time and temperature on physical, textural, and structural properties of yak meat. *Meat Sci.* 184, 108690 <https://doi.org/10.1016/j.meatsci.2021.108690>.
- Wen, W., Zhao, Z., Li, R., Guan, J., Zhou, Z., Luo, X., Suman, S.P., Sun, Q., 2019. Skeletal muscle proteome analysis provides insights on high altitude adaptation of yaks. *Mol. Biol. Rep.* 46 (3), 2857–2866. <https://doi.org/10.1007/s11033-019-04732-8>.
- Wu, J., Bond, C., Chen, P., Chen, M., Li, Y., Shohet, R.V., Wright, G., 2015. HIF-1 α in the heart: remodeling nucleotide metabolism. *J. Mol. Cell. Cardiol.* 82, 194–200. <https://doi.org/10.1016/j.yjmcc.2015.01.014>.
- Xiao, J., Wang, J., Gan, R., Wu, D., Xu, Y., Peng, L., Geng, F., 2022. Quantitative N-glycoproteome analysis of bovine milk and yogurt. *Curr. Res. Food. Sci.* 5, 182–190. <https://doi.org/10.1016/j.crf.2022.01.003>.
- Xin, J.-W., Chai, Z.-X., Zhang, C.-F., Zhang, Q., Zhu, Y., Cao, H.-W., Ji, Q.-M., Zhong, J.-C., 2019. Transcriptome profiles revealed the mechanisms underlying the adaptation of yak to high-altitude environments. *Sci. Rep.* 9 (1), 7558. <https://doi.org/10.1038/s41598-019-43773-8>.
- Xing, T., Wang, C., Zhao, X., Dai, C., Zhou, G., Xu, X., 2017. Proteome analysis using isobaric tags for relative and absolute analysis quantitation (iTRAQ) reveals alterations in stress-induced dysfunctional chicken muscle. *J. Agric. Food Chem.* 65 (13), 2913–2922. <https://doi.org/10.1021/acs.jafc.6b05835>.
- Xu, Z., Shao, Y., Liu, G., Xing, S., Zhang, Z., Zhu, M., Xu, Y., Wang, Z., 2021. Proteomics analysis as an approach to understand the formation of pale, soft, and exudative (PSE) pork. *Meat Sci.* 177, 108353 <https://doi.org/10.1016/j.meatsci.2020.108353>.
- Yang, F., Shen, Y., Camp, D.G., Smith, R.D., 2012. High-pH reversed-phase chromatography with fraction concatenation for 2D proteomic analysis. *Expert Rev. Proteomics* 9 (2), 129–134. <https://doi.org/10.1586/epr.12.15>.
- Yang, R., Geng, F., Huang, X., Qiu, N., Li, S., Teng, H., Chen, L., Song, H., Huang, Q., 2020. Integrated proteomic, phosphoproteomic and N-glycoproteomic analyses of chicken eggshell matrix. *Food Chem.* 330, 127167 <https://doi.org/10.1016/j.foodchem.2020.127167>.
- Yang, Y., Han, L., Yu, Q., Gao, Y., Song, R., Zhao, S., 2020. Phosphoproteomic analysis of longissimus lumborum of different altitude yaks. *Meat Sci.* 162, 108019 <https://doi.org/10.1016/j.meatsci.2019.108019>.
- Yang, Y., Yang, J., Ma, J., Yu, Q., Han, L., 2021. ITRAQ-mediated analysis of the relationship between proteomic changes and yak longissimus lumborum tenderness over the course of postmortem storage. *Sci. Rep.* 11 (1), 10450 <https://doi.org/10.1038/s41598-021-90012-0>.
- Zhang, H., Guo, T., Li, X., Datta, A., Park, J.E., Yang, J., Lim, S.K., Tam, J.P., Sze, S.K., 2010. Simultaneous characterization of glyco- and phosphoproteomes of mouse brain membrane proteome with electrostatic repulsion hydrophilic interaction chromatography. *Mol. Cell. Proteomics* 9 (4), 635–647. <https://doi.org/10.1074/mcp.M900314-MCP200>.
- Zuo, H., Han, L., Yu, Q., Guo, Z., Ma, J., Li, M., La, H., Han, G., 2018. Proteomic and bioinformatic analysis of proteins on cooking loss in yak longissimus thoracis. *Eur. Food Res. Technol.* 244 (7), 1211–1223. <https://doi.org/10.1007/s00217-018-3037-0>.
- Zuo, H., Han, L., Yu, Q., Niu, K., Zhao, S., Shi, H., 2016. Proteome changes on water-holding capacity of yak longissimus lumborum during postmortem aging. *Meat Sci.* 121, 409–419. <https://doi.org/10.1016/j.meatsci.2016.07.010>.